Self-assembled lyotropic liquid crystal gel for osteoarthritis treatment via anti-inflammation and cartilage protection

Liling Mei[a, #], Hui Wang[a, #], Jintian Chen[a, #], Ziqian Zhang[a], Feng Li[a], Yecheng Xie[a], Ying Huang[b], Tingting Peng[b, *], Guohua Cheng [b, *], Xin Pan[a], Chuanbin Wu[b]

[a] School of Pharmaceutical Sciences, Sun Yat-sen University, Guangzhou 510006, PR China

[b] College of Pharmacy, Jinan University, Guangzhou 510632, PR China

[#] These authors contributed equally to this work.

[*] Corresponding author:

Guohua Cheng, Professor

Tel.: +862013302203098; Fax: +862039943115

E-mail: ghcheng661203@126.com

College of Pharmacy, Jinan University, Guangzhou 510632, PR China

Tingting Peng, Ph.D.

Tel.: +862039943427; Fax: +862039943115

E-mail: pengtt@jnu.edu.cn

College of Pharmacy, Jinan University, Guangzhou 510632, PR China

Supporting information

1.1 Materials and animals

Glyceryl monooleate (GMO, DIMODAN®MO/D, 98 wt% monoglycerides, 1.5 wt% diglycerides, 0.4 wt% free fatty acids) was provided by Danisco Cultor (Brabrand, Denmark). CLX (purity ≥ 99.0%), commercial sodium hyaluronate injection (ARTZ®Dispo, 10 mg/mL sodium hyaluronate, Japan), and radioactive fluorine 18-fluorodeoxyglucose (^{18}F-FDG) were purchased from Guangzhou isotope atoms Hi-tech Pharmaceuticals Co., Ltd (Guangzhou, China). The PGE2 ELISA kit was obtained from Abcam Corporation (Cambridge, UK). The Milliplex multiple assay kit for analysis of IL-1β, IL-6 and TNF-α was procured from the EMD Mllipore Corporation (Massachusetts, USA). All other chemicals were of analytical grade and used as received.

Animals: Sprague-Dawley rats were purchased from the Guangdong Medical Laboratory Animal Center. All animal experiments were conducted in accordance with the guidelines approved by the Institutional Animal Care and Ethics Committee of Sun Yat-Sen University (approval No. IACUC-DD-18-0101)

1.2 Preparation of the LLC and HLC precursors

Based on the ternary phase diagram of GMO-EtOH-Water (Fig. S1), the ratio of GMO and ethanol in the range of 8:2~6:4 (w/w) could allow the LLC precursor to undergo a lamellar-hexagonal-cubic phase transition, which is beneficial for forming self-assembled gel. Therefore, we further used these formulation components to prepare LLC precursors with different CLX loading and studied their drug release behavior. As displayed in Fig. S2, the drug release behavior was affected by the ratio of GMO and ethanol, as well as the drug loading. Taken into account of the burst release and long-term cumulative release, the ratio of GMO and ethanol at 7: 3 (w/w) and 2wt% drug loading were selected to prepare LLC and HLC precursors for further study.

Specifically, the LLC precursor was prepared by dissolving GMO in preheated

ethanol (45 ± 0.5 °C) containing 2wt% CLX at a ratio of 7: 3 (w/w), followed by vortex and ultra-sonication. Hyaluronic acid (HA) is clinically used as a viscosupplementation for osteoarthritis (OA) therapy [1], and the simulated synovial fluid contains 3.4 mg/mL of HA [2, 3]. Therefore, the HA powder at a final concentration of 3.4 mg/mL was added to the LLC matrix to prepare HLC precursor and to simulate synovial fluid. Equivalent CLX incorporated in the commercially available product, ARTZ® containing 10 mg/mL HA, was formulated as a control. Besides, HA solution (HA 3.4) at a concentration of 3.4 mg/mL was self-made by dispersing HA powder into deionized water and used as a control.

1.3 Phase transition study

The phase transition from precursor solution to gel upon contacting water was evaluated by the polarized light microscopy (PLM; Micro-shot Technology Co., Ltd, Guangzhou, China) and small angle X-ray scattering (SAXS; SAXSee, Anton Paar, UK). The detailed procedures were carried out based on a previous literature [4].

1.4 *In vitro* drug release behavior

A dialysis method was adopted to study the release performance of different formulations. Briefly, CLX loaded formulations (ARTZ, LLC precursor, and HLC precursor) were added to the dialysis bags (MWCO = 1500 kDa), which were subsequently sealed and immersed in 10 mL of pH 7.4 PBS containing 0.5% Tween 80. Then, the tubes were placed in a steam bath shaker under 100 rpm and 37 °C. At predetermined intervals, the release buffer was completely withdrawn and replenished with equivalent fresh buffer. The amount of released CLX was determined by the high performance liquid chromatography (UV-2600, Shimadzu Co., Ltd., Japan) using Inert Sustain C-18 column (4.6 inner diameter x 150mm length, GL Sciences). The release kinetics of CLX from different formulations were fitted into different release mechanisms, including the Zero-order, First-order, Higuchi, Hixson crowell and

Ritger-peppa's kinetics equation.

1.5 Rheological tests

1.5.1 Viscosity test

The viscosity of HA, ARTZ, the LLC and HLC at both precursor and gel state, was determined using a Kinexus lab^{+} rotational rheometer (Malvern, UK) with a cone and plate (CP 1/60, 60 mm diameter and 1° cone angle) measuring system. The tests were performed at a temperature of 25 °C or 37 °C, and varying shear rate ranging from 0.01 s^{-1} to 100 s^{-1}. Viscosity curves were plotted as a function of shear rate.

1.5.2 Oscillation test

Oscillation sequence was conducted to evaluate the moduli (elastic modulus G' and viscous modulus G") of different formulations at different amplitude and frequency. The shear frequency varied from 0.1 Hz to 10 Hz and the amplitude was from 0.1% to 500%. Temperature was set at 37 C and plate PU 60 was selected for the tests. Moduli curves were plotted as a function of frequency or amplitude.

1.5.3 Thixotropy test

Thixotropy sequence was performed to evaluate the thixotropy property. The shear rate shifted from 0.1 s^{-1} (for 60 s) to 100 s^{-1} (for 30 s) and back to 0.1 s^{-1} (for 90 s). Temperature was set at 37 °C and plate CP 1/60 was selected for the tests. Viscosity curves were plotted as a function of time.

1.5.4 Large amplitude oscillatory shear test

Large amplitude oscillatory shear (LAOS) sequence was conducted to simulate the joint deflection and oscillation of articular surface during movement [2], where the

deformation of synovial fluids could be up to 1000% (ref) at frequency varying from 1 rad/s to 9 rad/s. In this test, cyclic strain was applied to ARTZ or HLC controlled by the test sequence and the output stress was recorded and analyzed. The strain and frequency were set at 1000% and 1.9 Hz (10 rad/s), respectively. The tests were conducted using plate CP 1/60 at 37 °C. Sinusoidal shear strain in a fixed frequency was applied during the test and the shear stress was recorded. Bowditch–Lissajous curves and Fourier transform rheology method were introduced to analyze the raw data of LAOS test.

1.6 Bio-distribution analysis

To study the *in vivo* drug distribution, Cy5 loaded formulations and their drug release profiles were prepared as the same method described for those of CLX. The bio-distribution and retention time in the articular cavity of Cy5 from different formulations were investigated by the *in vivo* near infrared (NIR) imager (LB98, Berthold Technologies, Germany) [5-7]. Briefly, fifteen Sprague-Dawley rats (weighing 200 ± 20 g), were randomly dived into five group, and anesthetized with 3% sodium pentobarbital (1.5 mL/kg) through intraperitoneal injection. 75 μL of saline, HA3.4, ARTZ, LLC and HLC loading equivalent Cy5, was directly injected into the left knee. At 0.08, 1, 4, 8, 12, 24, 48, 96, 168 h post-injection, the rats were imaged by the NIR living imager. The recorded images and fluorescence intensity within the joint cavity and the whole body were analyzed by the software. The ratio of fluorescent intensity in the joint cavity to the total, was also calculated to evaluate the retention ability.

1.7 Pharmacodynamics study

1.7.1 Establishment of OA model

OA-induced animal models were established on the SD rats (150 ± 20 g) by the modified hulth method [8, 9]. Briefly, the SD rats were anesthetized with 3%

pentobarbital at a dose of 1.5 mL/kg and received medicinal alcohol disinfection. The right knee was split through lateral parapatellar arthrotomy to achieve the optimal visualization of the ACL. The anterior cruciate ligament was cut off and two-thirds of the medial meniscus was resected with a scalpel. The joint was sutured layer by layer using 4-0 polydioxanone suture. After surgery, the rats received 40000 U penicillin through intramuscular injection every day for 1 weeks. The surgery-treated rats were kept in cages with free movement for 12 weeks to establish the OA model, which was confirmed by the positron emission tomography/computed (PET/CT) imaging and H&E staining.

1.7.2 PET/CTimaging

At 12 weeks for surgery, the inflammation in OA knees before and after IA injection of different formulations were examined by the PET/CT imaging with radioactive ^{18}F-FDG [10]. The OA rats were randomly divided into three groups, anesthetized and intravenously injected with ^{18}F-FDG (1 mCi/kg body weight). Both the OA model knees (right) and healthy control knees (left) of the rats were scanned with a Siemens Inveon PET/CT system (Siemens, Germany) for 20 min, using the following imaging parameters: 80 kV, 500 μA, 0.776 mm Pixel spaces, 0.796 mm slices, 128 *159 * 128 counts.

After scanning, 50 μL of saline, LLC precursor and HLC precursor was directly injected into the OA knees, respectively. At 7 and 14 days post-injection, the rats were anesthetized and scanned to evaluate the anti-inflammation efficacy of these formulations. The ^{18}F-FDG PET/CT images were converted into three-dimensional (3D) reconstructions according to an iterative 3D ordered subset expectation maximization algorithm (OSEM). Subsequently, the radiation signal within the regions of interest (ROI) drawn around the patellar cartilage was calculated. The quantitative evaluation of ^{18}FDG PET/CT imaging was performed by the normalized radiation. The quantitative index is calculated by the ratio of ^{18}FDG concentration in the OA (right) to that in the healthy (left) knee. The radiation signal concentrated within the left knee was set as the calibration to eliminate the ^{18}FDG absorb variation among the rats. The higher

normalized radiation indicated more severe inflammatory. Moreover, the visual analysis of the knees in the transaxial, coronal, and sagittal view was performed, respectively.

1.7.3 Cytokine quantification

The OA-induced SD rats with different treatments were anesthetized to collect the blood samples from orbital vein at 1, 3, 7, 14, and 21 days post-injection. The blood was centrifuged at 4000 rpm to obtain plasma. The cytokine quantification was conducted following the instructions of the ELISA kit for PGE2, and the Milliplex Multiple Assay kit for IL-1β, IL-6 and TNF-α.

1.7.4 Morphology evaluation and histological study

After administration for 21 days, the rats were sacrificed to collect the knee joints for visual inspection and histological evaluation of the repair of articular cartilage. Morphology evaluation was carried out by visual inspection using camera (Nikon D5200), while the histological assessment was conducted through hematoxylin-eosin (H&E) and safranin O-fast green staining [11]. Each specimen was sagittally sectioned into a 6-μm slice, and photographed using a microscopy. The histologic sections were further quantitatively evaluated using the Mankin score by two blinded observers [5].

1.8 *In vivo* degradation properties of LLC gel

To track the dynamic degradation performance of LLC gel, GMO was labelled with triiodobenzoic aci (TIBA) for CT imaging [12, 13]. TIBA-GMO was synthesized by acyl chlorination of TIBA and subsequent acylation of GMO with the resultant TIBA chloride. Briefly, TIBA (10.0 g, 20 mmol) was dissolved in dichloromethane (100 mL), followed by adding a catalytic amount of dimethylformamide (10 mg, 0.14 mmol). An excess of oxalyl chloride (10 mL, 79 mmol) was added dropwise and the mixture was stirred for 48 h at room temperature. Volatiles were evaporated under reduced pressure and the sedimentation was stripped with toluene three times to yield TIBA chloride. The hydroxyl end-group (OH) of GMO was further acetylated with TIBA chloride at

molar ratio of OH / chloride groups = 4, resulting in single hydroxyl end-group of GMO acetylated and the other free. The excess amount of GMO and the resultant GMO-TIBA were separated by silica gel column chromatography. The chemical structure of GMO, TIBA and GMO-TIBA were characterized with ^{1}H NMR using a Bruker AvanceIII, operating at 400 MHz. GMO and TIBA were dissolved in $CDCl_3$, while GMO-TIBA was dissolved in DMSO-D6.

To longitudinally trace the degradation of the LLC matrix, six healthy SD rats (weighing 200 ± 20 g) were subjected to Micro-CT scan at predetermined time intervals (Day 1, 4, 7 and 14) after IA injection of LLC matrix containing TIBA-GMO conjugate. The Micro-CT scan was performed in CT modality on Siemens Inveon PET/CT (Siemens, Germany) with following parameters: voltage of 80 kV, current of 500 μA, scan time of 25 min, field of view 61.13*40.75 mm^2 with 2-bed, slice thickness of 0.07959 mm, slice count 512, row count 768 and column count 768. CT images were converted into 3D reconstructions using the OSEM software. Subsequently, the TIBA signal within ROI, which was directly drawn around the visible gel in the reconstructed images, was calculated. The attenuation and the volume of the gel were also investigated for further analysis.

1.9 Biocompactibility

Healthy male rats were randomly divided into 4 groups (n = 8), and were intra-articularly injected with 75 μL of saline, ARTZ, LLC and HLC, respectively. After administration, the joint mobility was observed, and the diameter of joint was measured by vernier caliper to assess the degree of joint swelling. At day 1, 3, 7 and 14 post-administration, rats were sacrificed to strip the joints for histopathological inspection. The joints were sliced and embedded for H&E and safranin O-fast green staining to detect the physiological and pathological changes.

1.10 Statistical analysis

Statistical analyses were performed on DAS 2.0 software (Chinese

Pharmacological Association, Anhui, China). For comparing two groups, unpaired Students' t-test was used. The one-way ANOVA post Tukey analysis performed by SPSS software (SPSS version 19.0; SPSS Inc., Chicago, USA) was used to compare the significant difference among multiple groups. $P < 0.05$ was considered to be significantly different. All results were expressed as mean ± standard deviation.

2 Results

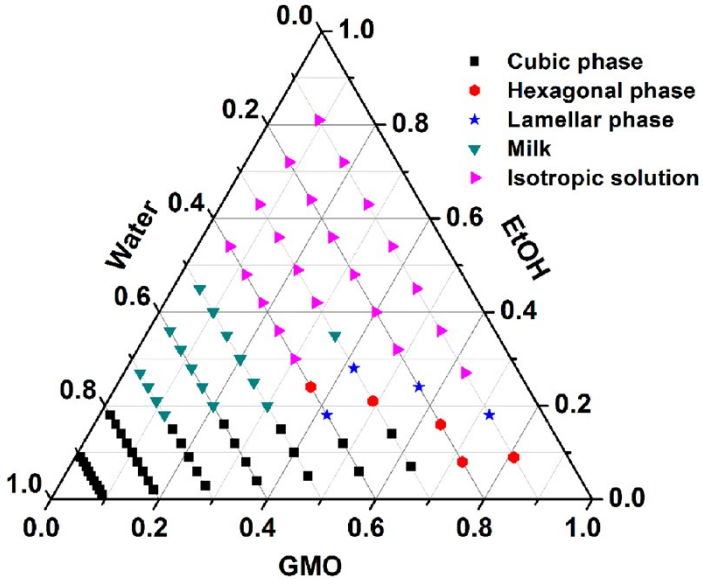

Fig.S1 Ternary phase diagram of GMO-EtOH-Water

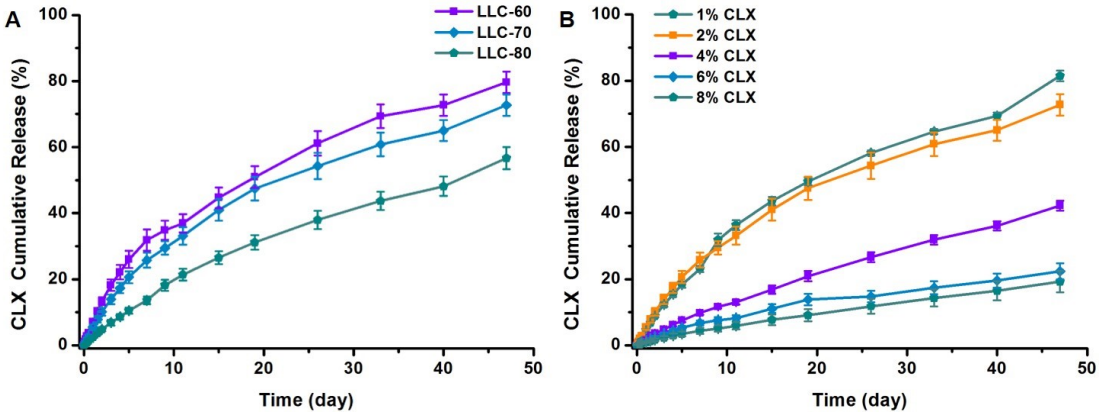

Fig.S2 The influence of GMO/EtOH ratios (A) and drug loading (B) on the drug release behavior (pH 7.4 PBS + 0.5% tween-80, 100 rpm, 37 ± 0.5°C, $n = 3$)

Table S1 Fitting of CLX release data from ARTZ, LLC and HLC into different release mechanism models (n=3)

	Model	Fitting equation	R^2
ARTZ	Zero-order	$y = kt + a$	0.8800
	First-order	$\ln(100-y) = kt + a$	0.9064
	Higuchi	$y = kt^{\wedge 1/2} + a$	0.7440
	Hixson crowell	$(100-y)^{\wedge 1/3} = kt + a$	0.8978
	Ritger-peppas	$y = kt^n$	**0.9825**
LLC	Zero-order	$y = kt + a$	0.9780
	First-order	$\ln(100-y) = kt + a$	**0.9971**
	Higuchi	$y = kt^{\wedge 1/2} + a$	0.9723
	Hixson crowell	$(100-y)^{\wedge 1/3} = kt + a$	0.9926
	Ritger-peppas	$y = kt^n$	0.9948
HLC	Zero-order	$y = kt + a$	0.9832
	First-order	$\ln(100-y) = kt + a$	**0.9977**
	Higuchi	$y = kt^{\wedge 1/2} + a$	0.9659
	Hixson crowell	$(100-y)^{\wedge 1/3} = kt + a$	0.9944
	Ritger-peppas	$y = kt^n$	0.9931

Table S2 Change of joint diameters at predetermined time intervals after IA injection of different formulations (n = 3)

Treatment	Joint diameter (mm)			
	Day 1	Day 3	Day 7	Day 14
Saline	9.01 ± 1.22	9.55 ± 2.06	9.65 ± 1.42	9.39 ± 1.84
ARTZ	8.86 ± 1.71	10.04 ± 1.86	9.25 ± 1.44	9.30 ± 1.84
LLC	10.21 ± 0.97	10.81 ± 1.64	10.73 ± 0.85	10.49 ± 0.82

HLC	9.45 ± 2.01	10.92 ± 2.74	11.05 ± 1.98	10.85 ± 2.11

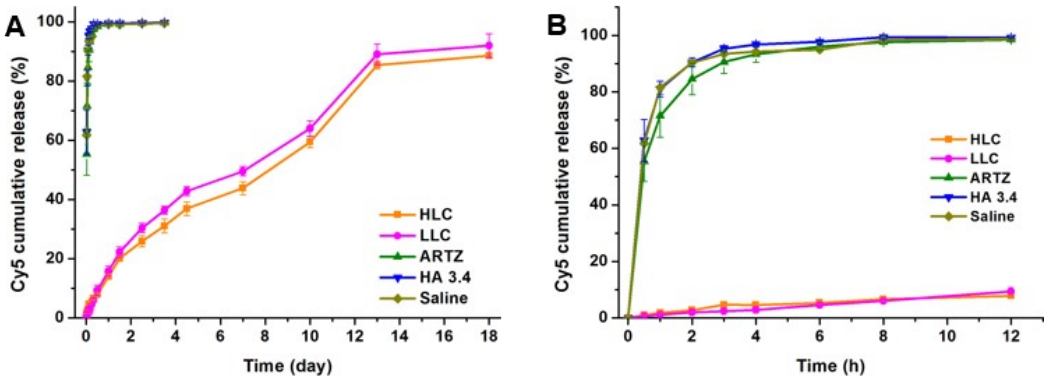

Fig.S3 *In vitro* release profiles of Cy5 from different formulations immersed in 40% DMSO dissolution buffer and performed at 37 ± 0.5°C and 100 rpm in an air bath shaker (n = 3): (A) Cumulative drug release over 18 days, and (B) Cumulative drug release in initial 12 h

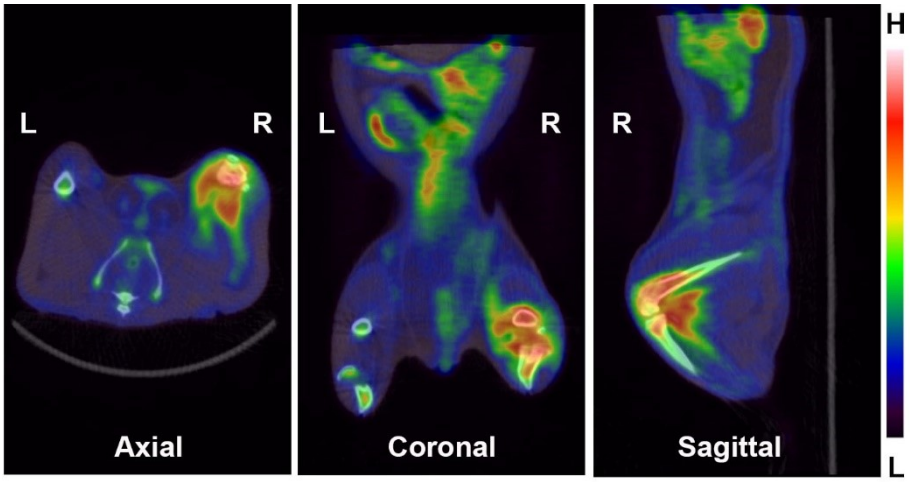

Fig. S4 The 3D PET/CT images of OA model animals before treatment: (A) Axial, (B) Coronal, (C) Sagittal.

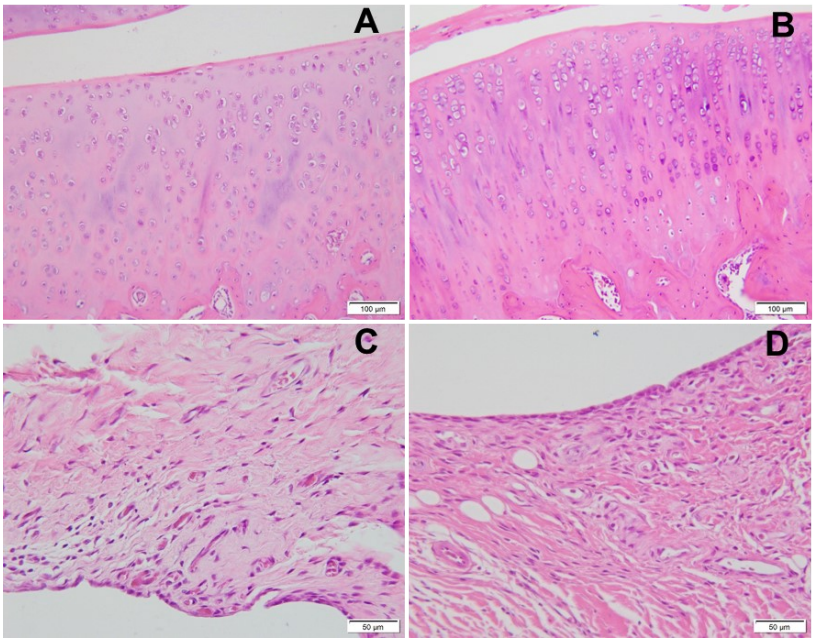

Fig. S5 H&E staining images of articular cartilage and synovium in OA-induced and healthy knee joints. The articular cartilage of OA-induced joints (A) and healthy joints (B). The articular synovium of OA-induced joints (C) and healthy joints (D).

References

[1] Y. Henrotin, R. Raman, P. Richette, H. Bard, J. Jerosch, T. Conrozier, X. Chevalier, A. Migliore. Consensus statement on viscosupplementation with hyaluronic acid for the management of osteoarthritis. Semin Arthritis Rheum 2015, 45 (2):140-149.

[2] Z. Zhang, G.F. Christopher. The nonlinear viscoelasticity of hyaluronic acid and its role in joint lubrication. Soft Matter 2015, 11(13):2596-2603.

[3] Z. Zhang, S. Barman, G.F. Christopher. The role of protein content on the steady and oscillatory shear rheology of model synovial fluids. Soft Matter 2014, 10(32):5965-5973.

[4] L.L. Mei, Y.C. Xie, Y. Huang, B. Wang, J.T. Chen, G.L. Quan, X. Pan, H. Liu, L.L. Wang, X.G. Liu, C.B. Wu. Injectable in situ forming gel based on lyotropic liquid crystal for persistent postoperative analgesia. Acta Biomaterialia 2018, 67:99-110.

[5] I. Rudnik-Jansen, S. Colen, J. Berard, S. Plomp, I. Que, M. van Rijen, N. Woike, A. Egas, G. van Osch, E. van Maarseveen. Prolonged inhibition of inflammation in

osteoarthritis by triamcinolone acetonide released from a polyester amide microsphere platform. J Control Release 2017, 253:64-72.

[6] M.J. Sandker, L.F. Duque, E.M. Redout, A. Chan, I. Que, C.W.G.M. Lowik, E.C. Klijnstra, N. Kops, R. Steendam, R. van Weeren, W.E. Hennink, H. Weinans. Degradation, intra-articular retention and biocompatibility of monospheres composed of PDLLA-PEG-PDLLA -b-PLLA multi-block copolymers. Acta Biomaterialia 2017, 48:401-414.

[7] T.K. Mwangi, I.M. Berke, E.H. Nieves, R.D. Bell, S.B. Adams, L.A. Setton. Intra-articular clearance of labeled dextrans from naive and arthritic rat knee joints. J Control Release 2018, 283:76-83.

[8] P. Chen, S. Zhu, Y. Wang, Q. Mu, Y. Wu, Q. Xia, X. Zhang, H. Sun, J. Tao, H. Hu. The amelioration of cartilage degeneration by ADAMTS-5 inhibitor delivered in a hyaluronic acid hydrogel. Biomaterials 2014, 35(9):2827-2836.

[9] P. Chen, C. Xia, S. Mei, J. Wang, Z. Shan, X. Lin, S. Fan. Intra-articular delivery of sinomenium encapsulated by chitosan microspheres and photo-crosslinked GelMA hydrogel ameliorates osteoarthritis by effectively regulating autophagy. Biomaterials 2016, 81:1-13.

[10] D.W. Townsend. Combined positron emission tomography–computed tomography: the historical perspective. Semin Ultrasound CT MRI 2008, 29(4):232-235.

[11] L. Yang, Y. Liu, X. Shou, D. Ni, T. Kong, Y. Zhao. Bio-inspired lubricant drug delivery particles for the treatment of osteoarthritis. Nanoscale 2020, 12(32):17093-17102.

[12] C. Zaharia, T. Zecheru, M.F. Moreau, F. Pascaretti-Grizon, G. Mabilleau, B. Marculescu, R. Filmon, C. Cincu, G. Staikos, D. Chappard. Chemical structure of methylmethacrylate-2-[2′, 3′, 5′-triiodobenzoyl] oxoethyl methacrylate copolymer, radio-opacity, in vitro and in vivo biocompatibility. Acta biomaterialia 2008, 4(6):1762-1769.

[13] M.J. Sandker, A. Petit, E.M. Redout, M. Siebelt, B. Müller, P. Bruin, R. Meyboom, T. Vermonden, W.E. Hennink, H. Weinans. In situ forming acyl-capped PCLA–

PEG–PCLA triblock copolymer based hydrogels. Biomaterials 2013, 34(32):8002-8011.